MJFAS
Malaysian Journal of Fundamental and Applied Sciences

RESEARCH ARTICLE

Bias-Corrected ESM–Driven Rainfall Downscaling via Tweedie Compound Poisson–Gamma and LASSO for Local Climate Projection

Fatkhurokhman Fauzi[a,b]*, Anik Djuraidah[b], Anang Kurnia[b], Rochdi Wasono[b]

[a]Department of Statistics, Universitas Muhammadiyah Semarang, Semarang, Indonesia; [b] School of Data Science, Mathematics, and Informatics, IPB University, Bogor, Indonesia

Abstract Climate change has increased rainfall variability and intensified the need for reliable local rainfall projections, particularly in agricultural regions such as West Java. Earth System Models (ESMs) provide useful climate change information but remain limited by coarse spatial resolution and systematic bias when applied to local-scale rainfall analysis. This study proposes an ESM-driven rainfall downscaling framework by integrating Tweedie Compound Poisson–Gamma with Least Absolute Shrinkage and Selection Operator (TCPG-LASSO), climate imprint-based resolution enhancement, and ISIMIP bias correction. Three ESMs, namely BNU-ESM, MIROC-ESM, and MIROC-ESM-CHEM, were evaluated using rainfall station data in West Java. Two modelling scenarios were compared: TCPG-LASSO without rescaling and bias correction and TCPG-LASSO with ESM rescaling and Inter-Sectoral Impact Model Intercomparison Project (ISIMIP) bias correction. Model performance was assessed using Taylor diagrams and time series plots. The results show that West Java rainfall follows a unimodal seasonal pattern and has a non-negative, positively skewed distribution, supporting the use of the TCPG framework. LASSO effectively selected a limited number of relevant ESM grids and reduced multicollinearity. The corrected TCPG-LASSO model provided better agreement with observed rainfall than the uncorrected model, with an average correlation of about 0.7. Among the evaluated ESMs, BNU-ESM showed the best performance and was used for six-month Standardized Precipitation Index (SPI-6) projection during 2021–2030. Across the 805 valid station-month SPI-6 values from June 2021 to December 2030, normal conditions dominated, with 583 occurrences. Dry and wet anomalies were also projected, including 85 moderately dry, 15 severely dry, 2 extremely dry, 55 moderately wet, 47 very wet, and 18 extremely wet occurrences. These findings demonstrate that the proposed framework can support drought monitoring, agricultural planning, and hydrometeorological disaster mitigation in West Java.

Keywords: Bias Correction; Earth System Model; Rainfall Downscaling; Standardized Precipitation Index; Tweedie Compound Poisson–Gamma; West Java.

***For correspondence:**
fatkhurokhmanf@unimus.ac.id

Received: 20 September 2025
Accepted: 10 July 2026

Introduction

Rainfall is essential for human life; lack and excess rain can cause hydrometeorological disasters. Increased extreme rainfall can trigger flash floods and landslides in densely populated areas [1]. A significant decrease in rainfall can cause drought; this often occurs in Indonesia during the El Nino period, impacting the agricultural and clean water sectors [2]. Purnamasari et al. [3] found that the El Nino event increases the potential for drought in West Java. Tropical areas with low rainfall and poor soil moisture make them vulnerable to extreme drought.

In addition to El Nino and La Nina, rainfall is also affected by climate change phenomena. Significant changes in rainfall patterns due to climate change can seriously impact crop production. Global studies show that drought can significantly reduce crop yields such as corn, wheat, soybeans, and rice, with losses reaching USD 166 billion [4], [5]. In Africa, the projected risk of crop failure due to drought under climate change scenarios will double by 2100. Projections of future rainfall under climate change scenarios are crucial to mitigate hydrometeorological disasters.

Earth System Models (ESM) are future climate change simulation models. This model simulates the interaction between global warming and the influence of the carbon cycle on biogeochemistry [6]. The climate change simulation contained in ESM follows the Representative Concentration Pathways (RCP) scenario. RCP projects future greenhouse gas concentrations with four scenarios, namely RCP2.6, RCP4.5, RCP6, and RCP8.5. Of the four scenarios, the difference is the level of radiative forcing. Most studies on climate change in Indonesia using ESM have been conducted (e.g., [7], [8], [9]). However, ESM has a low resolution in explaining regional climate variability and has a significant bias. To increase the resolution of ESM, statistical downscaling and bias correction approaches are used [10], [11], [12].

Statistical Downscaling methods for predicting local rainfall based on global-scale ESM information have been widely used (e.g., [13], [14]). However, statistical downscaling methods still ignore the occurrence of no rain, which is the same phenomenon as rainy days. According to Dunn and Smyth [15], rainfall has two components: rainfall occurrence, which follows a discrete component and rainfall intensity, which follows a continuous component. The distribution that can accommodate both components is the Tweedie Compound Poisson Gamma (TCPG) [16], [17]. Statistical Downscaling research with the TCPG Regression approach includes [18], [19], [20].

Multicollinearity is one of the problems caused by ESM data due to the proximity between data grids. The effects caused by multicollinearity can cause the model to overfit, losing its ability to predict accurately [21]. Multicollinearity can also increase the Root Mean Squared Error (RMSE) and Root Mean Squared Error of Prediction (RMSEP) values, thereby reducing the quality of downscaling statistical predictions [22]. The Least Absolute Shrinkage and Selection Operator (LASSO) method is one solution to overcome multicollinearity problems on a large scale, such as ESM, through the L1 penalty [19], [21], [22]. The LASSO method with L1 regularization automatically selects important variables by reducing the coefficients of insignificant variables to zero, making the model easier to understand and the computational process more efficient [18], [23].

The uniqueness of the TCPG-LASSO approach lies in its ability to simultaneously address two important issues in rainfall statistical downscaling. The TCPG distribution is appropriate for rainfall data because it can accommodate both zero rainfall occurrence and positive, right-skewed rainfall intensity. Meanwhile, the LASSO penalty is able to select important ESM grid predictors and reduce multicollinearity among spatially correlated grids. Therefore, the TCPG-LASSO approach is particularly suitable for ESM-driven rainfall downscaling, where the response variable is non-normal and the predictor variables are highly correlated.

On a global scale, ESM still has a high bias, so increasing the resolution and correction of ESM is very important [7]. The developed bias correction methods are Quantile Mapping (QM) [24], [25], Quantile Delta Mapping (QDM) [26], Bias Correction Built Analogues with Quantile Mapping Reordering (BCCAQ) [27], and The Inter-Sectoral Impact Model Intercomparison Project (ISIMIP) [28]. Fauzi et al. [29] compared three bias correction methods for the Indonesian region, namely QDM, BCCAQ, and ISIMIP, and found that ISIMIP showed the best performance for rainfall variables. Therefore, this study uses the ISIMIP method for bias correction.

In previous studies, calibration of climate model outputs was commonly carried out using bias correction methods to adjust the distribution of model outputs to reference data, such as observations or reanalysis data, during the historical period. Methods such as Quantile Mapping, Quantile Delta Mapping, BCCAQ, and ISIMIP have been used to reduce systematic bias in climate model outputs. In general, these methods estimate the relationship between simulated and reference data in the historical period and then apply the correction function to future climate projections. Based on previous findings for rainfall variables in Indonesia, ISIMIP was selected in this study because it has shown good performance in correcting ESM rainfall bias.

Accordingly, the main contribution of this study is the integration of TCPG-LASSO statistical downscaling with ESM resolution enhancement using the climate imprint method and ISIMIP bias correction for local rainfall prediction in West Java. This framework differs from previous studies because it combines distribution-aware rainfall modelling, grid-based predictor selection, calibrated ESM information, and SPI-6-based seasonal drought and wetness projection within a single analytical framework.

Materials and Methods

This study uses rainfall data sources: observation data (stations), reanalysis, and climate change scenarios. Observation rainfall data (station) was obtained from the Meteorology, Climatology and Geophysics Agency (BMKG). Reanalysis data is sourced from the European Center for Medium-Range Weather Forecasts (ECMWF). Reanalysis data is generated by assimilating numerical data using atmospheric models and observation data from various sources, such as satellites. This study's climate change scenario data is the Representative Concentration Pathway (RCP) 4.5. RCP4.5 is a climate change scenario where atmospheric CO_2 concentration will reach 650 ppm in 2100. Globally, the RCP4.5 scenario estimates a temperature increase of 1.5°C to 2°C in 2100 compared to the pre-industrial era. This condition aligns with the current trend of increasing temperatures due to greenhouse gas emissions [30]. This study will focus on rainfall in West Java Province because the province is one of the national food producers. Data details are in Table 1.

Table 1. Research Data

Data	Scenario	Resolution	Institution	Scale
Rainfall station	Observational Data	-	BMKG	Monthly
Era-Interim	Reanalysis Data	$0.25° \times 0.25°$	ECMWF	Monthly
Beijing Normal University Earth System Model (BNU-ESM)	RCP4.5	$2.8° \times 2.8°$	Beijing Normal University	Monthly
Model for Interdisciplinary Research on Climate Earth System Model (MIROC-ESM)	RCP4.5	$2.8° \times 2.8°$	JAMSTEC	Monthly
MIROC-ESM with chemistry module (MIROC-ESM-CHEM)	RCP4.5	$2.8° \times 2.8°$	JAMSTEC	Monthly

This study uses three ESM outputs, namely BNU-ESM [31], MIROC-ESM, and MIROC-ESM-CHEM [32], as predictor variables in the statistical downscaling model. These ESMs were selected because they have been commonly used in climate studies over Asian and Indonesian regions and provide relevant climate information for rainfall projection. The performance of each ESM was evaluated, and the best-performing ESM was subsequently used to calculate the Standardized Precipitation Index (SPI) for drought assessment in West Java.

The conceptual framework of this study is designed to integrate ESM resolution enhancement, bias correction, and TCPG-LASSO statistical downscaling for local rainfall prediction in West Java. The framework begins with the preparation of three main datasets: observed rainfall data from BMKG, ERA-Interim reanalysis data, and ESM outputs from BNU-ESM, MIROC-ESM, and MIROC-ESM-CHEM. All datasets were first adjusted to the West Java spatial domain and harmonized on a monthly temporal scale. The ESM outputs, which originally have a coarse spatial resolution of $2.8° \times 2.8°$, were then rescaled to the $0.25° \times 0.25°$ resolution of ERA-Interim using the climate imprint method [33]. After the resolution enhancement process, the rescaled ESM data were bias-corrected using the ISIMIP method to reduce systematic differences between ESM outputs and reference climate data [28]. The overall conceptual framework and research stages are summarized in Figure 1.

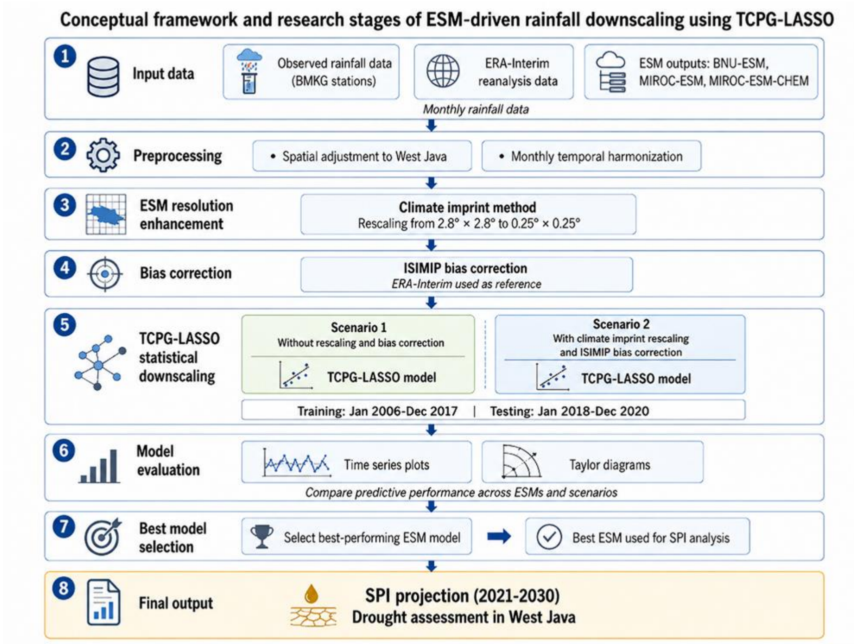

Figure 1. Conceptual framework and research stages of ESM-driven rainfall downscaling using TCPG-LASSO.

The statistical downscaling process was conducted using the TCPG-LASSO approach. The data were divided into two periods: January 2006 to December 2017 for training and January 2018 to December 2020 for testing. Two modelling scenarios were evaluated. The first scenario used TCPG-LASSO without rescaling and bias correction, while the second scenario used TCPG-LASSO with ESM rescaling and ISIMIP bias correction. This comparison was conducted to assess whether resolution enhancement and bias correction could improve the predictive accuracy of the TCPG-LASSO model. Model performance was evaluated using time series plots and Taylor diagrams. Finally, the best-performing ESM model was selected and used to calculate the SPI projection under the climate change scenario for drought assessment in West Java.

TCPG–Least Absolute Shrinkage and Selection Operator (LASSO)

Tweedie Compound Poisson Gamma (TCPG) is a distribution often used to model rainfall data that has mixed characteristics between discrete (rainfall events) and continuous (rainfall intensity) components. TCPG can capture the zero-inflated (many zero values) and highly skewed distributions. This model is helpful in Statistical Downscaling (SD), where GCM output data is used to predict local rainfall. LASSO is used in TCPG to overcome multicollinearity in predictor data and select significant variables [19]**.** Let Y_i follow a Tweedie distribution with mean $\mu_i > 0$, dispersion parameter $\phi > 0$, and power parameter $1 < p < 2$. The mean rainfall is related to the predictor variables through a log-link function, $\log(\mu_i) = \boldsymbol{x}_i'\boldsymbol{\beta}$, $\mu_i = \exp(\boldsymbol{x}_i'\boldsymbol{\beta})$. For fixed values of p and ϕ, the kernel of the Tweedie log-likelihood can be written as:

$$\ell(\boldsymbol{\beta}, p, \phi) = \sum_{i=1}^{n} \frac{1}{\phi}\left[\frac{y_i \mu_i^{1-p}}{1-p} - \frac{\mu_i^{2-p}}{2-p}\right] \quad (1)$$

The TCPG-LASSO estimator is then obtained by minimizing the average negative log-likelihood with an L_1 penalty:

$$\widehat{\boldsymbol{\beta}}_\lambda = \arg\min_{\beta}\left\{-\frac{1}{n}\ell(\boldsymbol{\beta}, p, \phi) + \lambda \sum_{j=1}^{q} |\boldsymbol{\beta}_j|\right\} \quad (2)$$

Here, n denotes the number of observations, q is the number of ESM grid predictors, $\boldsymbol{\beta}$ is the vector of regression coefficients, and $\lambda \geq 0$ is the LASSO tuning parameter. The intercept is not penalized. Increasing λ produces stronger coefficient shrinkage and may set some coefficients exactly to zero, thereby selecting relevant ESM grid predictors and reducing multicollinearity [18]. Through this formulation, TCPG-LASSO can simultaneously accommodate the non-negative and right-skewed characteristics of rainfall and perform predictor selection.

TCPG-LASSO has been used to predict rainfall characteristics in various geographic locations, including seasonal rainfall patterns. Studies have shown that this model is superior to traditional linear regression methods in predicting rainfall intensity and frequency. In addition, TCPG-LASSO can be applied in a bias correction approach, which improves prediction accuracy in areas with highly variable rainfall characteristics [20].

Inter-Sectoral Impact Model Intercomparison Project (ISIMIP) Bias Correction

The Inter-Sectoral Impact Model Intercomparison Project (ISIMIP) provides a framework for integrating climate model data into cross-sector impact simulations. A key component of ISIMIP is bias correction, which is used to adjust rainfall data from climate models to be consistent with historical observations. This process is critical because rainfall has high spatial and temporal variability, which affects projections of climate change impacts on sectors such as agriculture and water resources [34]. In this study, rainfall bias correction was implemented using the complete ISIMIP3BASD procedure described by Lange [28], rather than mean scaling alone. The correction functions were estimated by comparing the rescaled ESM data with the ERA-Interim reference data during the historical calibration period and were subsequently applied to the future RCP4.5 simulations. ISIMIP3BASD uses a trend-preserving parametric quantile-mapping framework to adjust biases across the precipitation distribution while retaining the climate-change signal simulated by the ESM. Therefore, the following mean-ratio expression is presented only as a simplified representation of the mean-adjustment component of the complete ISIMIP3BASD procedure:

$$P_{corr} = P_{raw} \cdot \frac{P_{obs_{mean}}}{P_{sim_{mean}}} \quad (3)$$

where P_{corr} denotes corrected precipitation, P_{raw} is the precipitation simulated by the ESM, $P_{obs_{mean}}$ is the mean precipitation from the ERA-Interim reference data, and $P_{sim_{mean}}$ is the mean precipitation from the rescaled ESM data [28].

Adjusting rainfall poses unique challenges, mainly because precipitation distributions are often non-normal and include significant zero values. ISIMIP addresses this using a percentile-based method that preserves the historical data distribution patterns while ensuring long-term trends remain intact. This method also ensures local-scale adjustments for high spatial variability [35].

Rainfall bias correction has been applied across various sectors, including hydrology and agriculture. In global hydrological simulations, bias correction ensures that extreme rainfall patterns are accurately represented, enabling more reliable river flow and flood risk predictions. In agricultural applications, correcting biases in growing-season rainfall can reduce errors in simulated crop yields and improve the reliability of projected yield changes under climate change [36].

Taylor Diagram

The Taylor Diagram is a graphical tool used to evaluate model performance by comparing simulation results with observational data. This diagram combines three key statistical metrics, Correlation Coefficient (r), Standard Deviation (σ), and Centred Root Mean Square Error (RMSEc), into a single polar plot. It is widely used in climatology, hydrology, and other fields to assess how well a model reproduces observed data's spatial or temporal patterns [37].

$$r = \frac{\sum_{i=1}^{n}(X_i - \bar{X})(Y_i - \bar{Y})}{\sqrt{\sum_{i=1}^{n}(X_i - \bar{X})^2 \sum_{i=1}^{n}(Y_i - \bar{Y})^2}} \quad (4)$$

$$\sigma = \sqrt{\frac{\sum_{i=1}^{n}(X_i - \bar{X})^2}{n}} \quad (5)$$

$$RMSE_c = \sqrt{\frac{\sum_{i=1}^{n}\left((X_i - \bar{X}) - (Y_i - \bar{Y})\right)^2}{n}} \quad (6)$$

This measures the pattern agreement between the simulation data Y and observations X. These formulas calculate the relative position of the model on the diagram, where points closer to the reference indicate better performance [38].

The Taylor Diagram plots the standard deviation as the radial distance and the correlation coefficient as the angle. The RMSEc is represented by the Euclidean distance from the model point to the reference point (perfect observation representation). This diagram allows for simultaneous comparison of multiple model performances with clear visual interpretation, making it easy to assess which model is the most accurate quickly [37].

Standardized Precipitation Index (SPI)

The Standardized Precipitation Index (SPI) is a statistical method used to monitor drought and measure rainfall anomalies quantitatively across various time scales. SPI is calculated based on the historical probability distribution of rainfall, which is transformed into a standard normal distribution, enabling comparisons across locations and periods. It is vital to understand drought and wet patterns in various applications, including agriculture, water resource management, and drought risk mitigation [39].

The computation of SPI involves fitting a two-parameter gamma distribution to a precipitation series. The resulting cumulative probability is then transformed into a standard normal variate. The cumulative probability of precipitation is then transformed using a standard normal distribution function. Let X denote accumulated precipitation over a specified time scale. Because the two-parameter gamma distribution is defined only for positive precipitation values, the probability of zero precipitation must be incorporated separately. The cumulative probability of precipitation is therefore expressed as:

$$\begin{aligned} H(x) &= q + (1-q)G(x;\alpha,\beta) \\ SPI &= \Phi^{-1}[H(x)] \end{aligned} \tag{7}$$

where q is the probability of zero precipitation, $G(x;\alpha,\beta)$ is the cumulative distribution function of the fitted gamma distribution, and are the shape α and β scale parameters, respectively, and Φ^{-1} is the inverse cumulative distribution function of the standard normal distribution. Consequently, negative SPI values indicate drier-than-normal conditions, whereas positive SPI values indicate wetter-than-normal conditions [39].

SPI can be calculated for different time scales, such as 1 month, 3 months, or 12 months, to identify short-term to long-term drought patterns. For instance, shorter time scales are helpful for agriculture, while longer time scales are relevant for water resource management**.** SPI values are categorized to identify the intensity of droughts or wet periods. The classification is as follows:

- $SPI \geq 2.0$: Extremely wet
- $1.5 \leq SPI < 2.0$: Very wet
- $1.0 \leq SPI < 1.5$: Moderately wet
- $-1.0 < SPI < 1.0$: Near normal
- $-1.5 < SPI \leq -1.0$: Moderately dry
- $-2.0 < SPI \leq -1.5$: Severely dry
- $SPI \leq -2.0$: Extremely dry

In this study, precipitation was accumulated over a 6-month time scale to obtain SPI-6, representing seasonal accumulated rainfall anomalies within the Indonesian wet–dry seasonal cycle. For each rainfall station, the gamma distribution parameters were estimated from the downscaled BNU-ESM rainfall projection series for 2021–2030, after which the cumulative probabilities were transformed into standard normal values using Equation (7). Positive SPI-6 values indicate wetter-than-normal conditions, whereas negative SPI-6 values indicate drier-than-normal conditions. The resulting SPI-6 values were subsequently classified into drought and wetness categories using the standard SPI classification. Because SPI-6 requires six consecutive months of precipitation, values for January–May 2021 were unavailable for category classification. Accordingly, the frequency analysis was based on 115 valid monthly SPI-6 values per station from June 2021 to December 2030, corresponding to 805 station-month occurrences across the seven stations.

Results and Discussion

Exploration of rainfall characteristics

West Java Province's rainfall is classified as a unimodal pattern, with one main wet peak and one dry trough within a year [18]. This pattern is closely related to the seasonal monsoon cycle. The northwest monsoon generally brings wetter conditions from November to March, while the southeast monsoon is associated with the drier period from May to November [40]. The seven rainfall stations analyzed in this study show a similar seasonal pattern, although the rainfall intensity and variability differ from one station to another.

Figure 2 shows that monthly rainfall at the seven stations generally ranges from nearly 0 to more than 1000 mm/month. Higher rainfall is mostly observed during the wet season, especially from January to March and again from November to December. In contrast, rainfall decreases during the dry season, particularly from June to September. This pattern is clearly visible in most stations, where the median rainfall during the dry months is much lower than during the wet months.

Pondok Salam, Wanayasa, and Gunung Mas show relatively higher rainfall intensity than the other stations, as indicated by the wider boxplots and higher upper values during several wet months. Purwakarta and Cibukamanah tend to have lower rainfall intensity, although their seasonal pattern remains consistent with the other stations. Several outliers are also found in different months, indicating the presence of extreme rainfall events. These anomalies may be related to interannual climate variability, including La Niña conditions, which can increase rainfall intensity during the transition season [41].

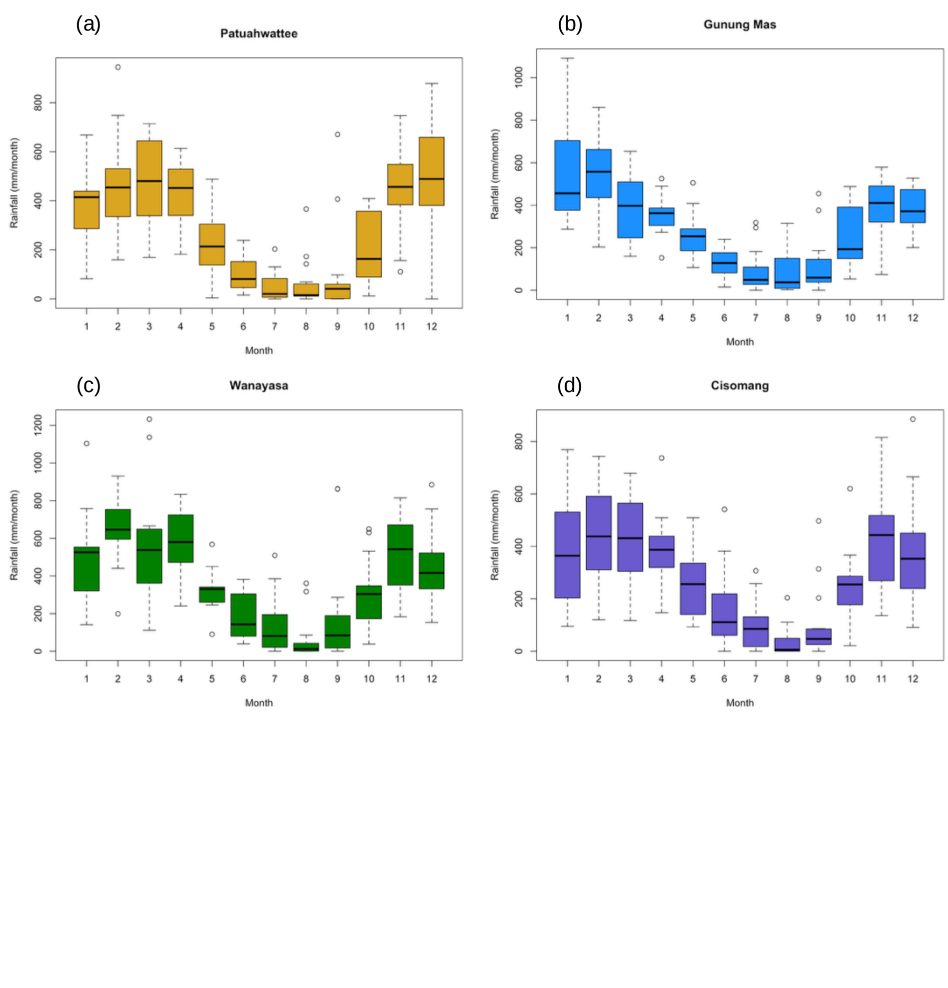

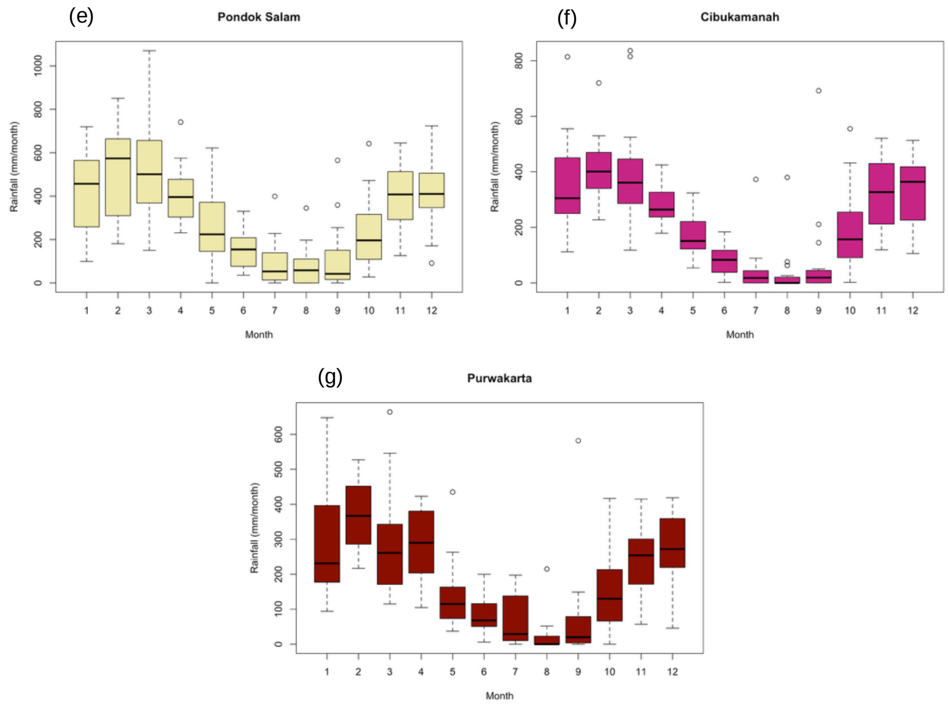

Figure 2. Boxplots of monthly rainfall at seven rainfall stations in West Java during 2006–2020: (a) Patuahwattee, (b) Gunung Mas, (c) Wanayasa, (d) Cisomang, (e) Pondok Salam, (f) Cibukamanah, and (g) Purwakarta.

The pattern shown in Figure 2 indicates that rainfall in the study area has strong seasonality and considerable variation across stations. The wet months are characterized by higher rainfall and wider variability, while the dry months show lower rainfall and more compact distributions. This characteristic is important for the next modelling stage because rainfall data are not normally distributed and may contain zero or near-zero values as well as extreme positive values.

Figure 3 shows the frequency distribution of monthly rainfall at the seven stations. In general, rainfall is distributed on non-negative values, with most observations concentrated at low to moderate rainfall levels and a long tail toward high rainfall intensity. This pattern indicates that rainfall data are positively skewed and do not follow a normal distribution. Several stations, such as Wanayasa, Pondok Salam, Gunung Mas, and Patuahwattee, show wider rainfall ranges, indicating higher rainfall variability. Meanwhile, Purwakarta and Cibukamanah tend to have lower rainfall intensity, although their distributions still show the same right-skewed pattern.

The high frequency of low rainfall values and the presence of extreme positive rainfall values indicate that rainfall data require a distribution that can accommodate both dry or very low rainfall conditions and positive rainfall intensity. A conventional gamma distribution can model positive rainfall values, but it is less suitable when rainfall data contain zero or near-zero observations. Therefore, modelling rainfall using the gamma distribution alone may not be sufficient to capture the full characteristics of the data. The Tweedie Compound Poisson-Gamma distribution is more appropriate because it combines a discrete component for rainfall occurrence and a continuous component for rainfall intensity [17].

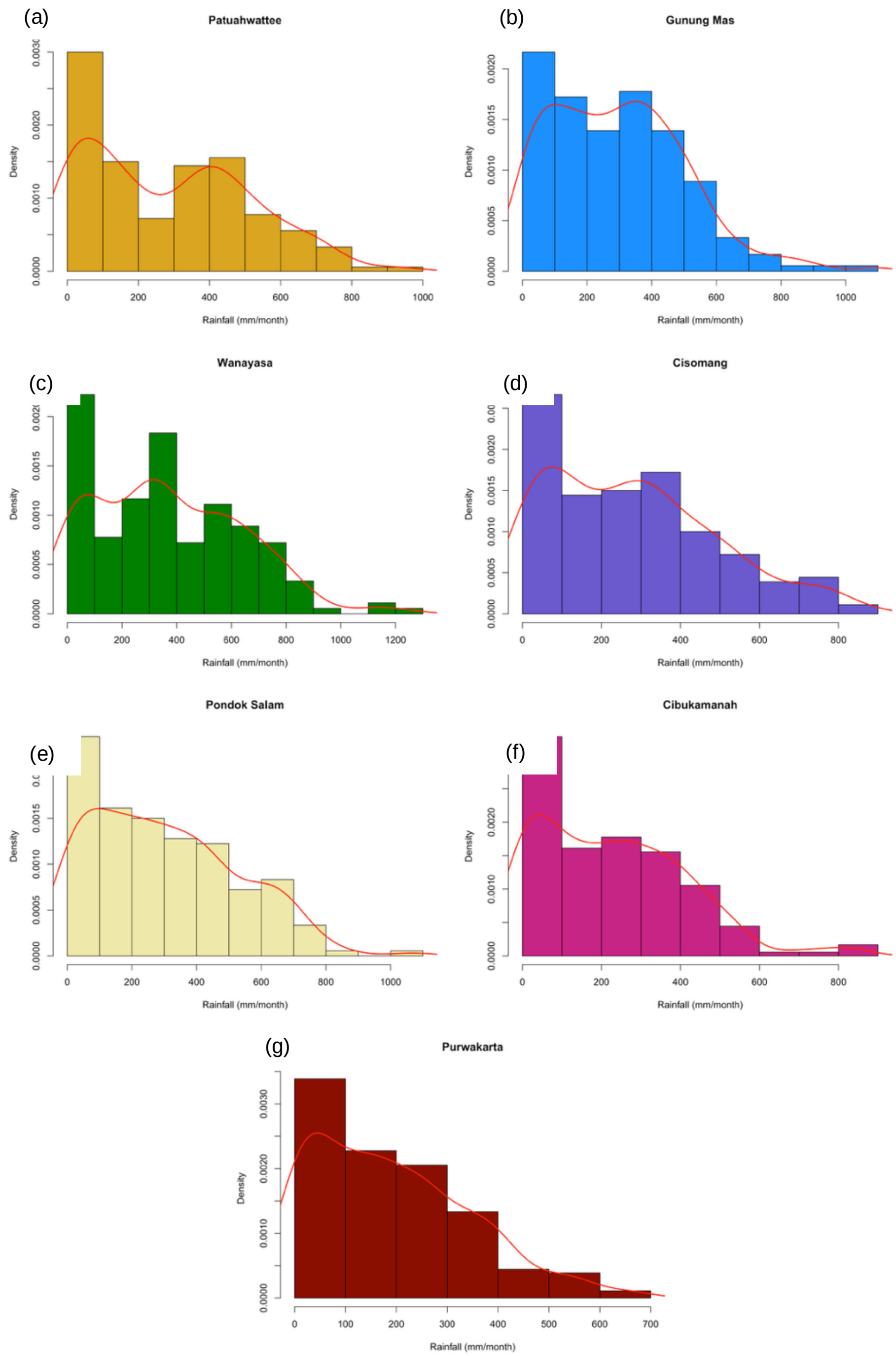

Figure 3. Frequency distribution and density curves of monthly rainfall at seven rainfall stations in West Java during 2006–2020: (a) Patuahwattee, (b) Gunung Mas, (c) Wanayasa, (d) Cisomang, (e) Pondok Salam, (f) Cibukamanah, and (g) Purwakarta.

The Tweedie distribution is defined by the variance power parameter p. For rainfall data that follow a Compound Poisson-Gamma structure, the parameter p lies in the interval $1 < p < 2$ [42]. In this study, the parameter p was estimated using the Maximum Likelihood Estimation (MLE) approach through profile likelihood. The estimated values and their 95% confidence intervals are presented in Table 2. The results show that the estimated p values for all seven stations fall within the interval $1 < p < 2$, indicating that monthly rainfall in West Java is consistent with the Tweedie Compound Poisson-Gamma distribution. These findings support the use of the TCPG framework for the statistical downscaling model in the next stage.

Table 2. p parameter estimation results

Station	p	Lower bound	Upper bound
Purwakarta	1.43	1.35	1.53
Cibukamanah	1.47	1.40	1.56
Pondok Salam	1.44	1.35	1.54
Cisomang	1.50	1.40	1.58
Wanayasa	1.51	1.42	1.61
Gunung Mas	1.58	1.48	1.71
Patuahwattee	1.62	1.55	1.71

The next step is to perform statistical downscaling using TCPG. This study uses two scenarios to determine the effectiveness of bias correction and scaling in increasing the accuracy of modelling results. In this study, the spatial resolution of the ESM data was enhanced using the climate-imprint method developed by Hunter and Meentemeyer [33]. This procedure rescaled the ESM outputs from their original spatial resolution of 2.8° × 2.8° to 0.25° × 0.25°, corresponding to the spatial resolution of ERA-Interim. The rescaled ESM data were subsequently bias-corrected using the ISIMIP procedure, with ERA-Interim reanalysis data from ECMWF serving as the reference. Previous evaluation for the Indonesian region showed that ISIMIP effectively reduced biases in rescaled rainfall data and produced correlations of approximately 0.4–0.5 with observational rainfall data [29]. The resulting high-resolution and bias-corrected ESM data were then used as predictor variables in the TCPG-LASSO model.

TCPG-LASSO for Predictor Selection

Multicollinearity and computational efficiency are challenges in statistical downscaling. ESM data in the form of intersecting grids cause this problem. ESM data before scaling consists of 9 grids; after scaling, it becomes 609 grids. Grid selection with a penalty using the LASSO method will prevent multicollinearity and make the computational process more efficient.

Table 3. Parameter of LASSO Penalty

Station	MIROC-ESM		BNU-ESM		MIROC-ESM-CHEM	
	Without	With	Without	With	Without	With
Purwakarta	91.17	9.16	33.05	18.96	10.83	6.34
Cibukamanah	8.52	6.16	39.35	15.55	16.98	17.76
Pondok Salam	103.83	13.64	14.65	20.50	5.01	6.57
Cisomang	15.25	17.25	17.58	16.95	11.07	4.86
Wanayasa	55.30	12.02	27.07	14.71	2.19	4.59
Gunung Mas	9.04	3.83	0.42	8.89	5.29	3.12
Patuahwattee	51.06	3.01	11.25	9.17	2.57	2.76

The number of grids selected in the TCPG-LASSO process is determined by the LASSO penalty parameter, denoted by λ. The penalty parameter was not determined by trial and error or simulation. In this study, the optimal λ value was selected using 10-fold cross-validation. A sequence of candidate λ values was evaluated, and for each λ value, the TCPG-LASSO model was fitted to the training data. The prediction deviance was then calculated across the validation folds. The optimal λ value was selected based on the minimum cross-validated deviance. Therefore, the selected penalty parameter represents the value that provides the best balance between model fit and predictor shrinkage. This procedure also determines the number of ESM grid predictors retained in the final TCPG-LASSO model. Table 3 shows that most λ values are higher before scaling and bias correction than after.

Table 4. Number of Selected ESM Grid Predictors

Station	MIROC-ESM		BNU-ESM		MIROC-ESM-CHEM	
	Without	With	Without	With	Without	With
Purwakarta	3	8	2	8	5	10
Cibukamanah	6	6	2	10	6	4
Pondok Salam	3	4	3	7	6	5
Cisomang	3	2	2	9	7	6
Wanayasa	3	5	3	13	6	9
Gunung Mas	6	6	4	9	7	8
Patuahwattee	3	7	3	11	7	8

Based on Table 4, the TCPG-LASSO model retained only a limited number of ESM grids, indicating a sparse predictor structure. In the model without scaling and bias correction, two to seven grids were selected from the original nine ESM grids. After scaling and bias correction, only a small subset of grids was retained from the 609 available grids. This result is expected because the LASSO penalty shrinks the coefficients of less informative predictors to zero and retains only grids that contribute substantially to reducing prediction deviance. In addition, many neighbouring ESM grids contain similar climate information due to spatial correlation; therefore, selecting all grids would increase multicollinearity and computational complexity without necessarily improving predictive performance. The selected grids generally represent the most relevant local climate information for each rainfall station, particularly grids located near the station or those with stronger predictive contribution.

TCPG-LASSO Performance Evaluation

TCPG-LASSO performance evaluation using the Taylor Diagram [37], [43]**.** The Taylor diagram provides a compact visual comparison of model performance by combining three statistical measures, namely the correlation coefficient (r), standard deviation (σ), and centred root mean square error (RMSE). In this study, the diagram was used to compare the performance of three ESM predictors, namely BNU-ESM, MIROC-ESM, and MIROC-ESM-CHEM, under two modelling scenarios: without scaling and bias correction and with scaling and bias correction. The orange point represents the observed rainfall data, and model points located closer to this reference point indicate better agreement with the observations.

Figure 4 shows that the performance of TCPG-LASSO varies among stations and ESM models. In general, the models with scaling and bias correction, represented by the plus symbols, tend to be closer to the observation point than the models without scaling and bias correction. This indicates that the combination of climate imprint rescaling and ISIMIP bias correction improves the ability of ESM outputs to represent local rainfall variability. The improvement can be observed from the relatively higher correlation values and the standard deviation values that become closer to those of the observed data.

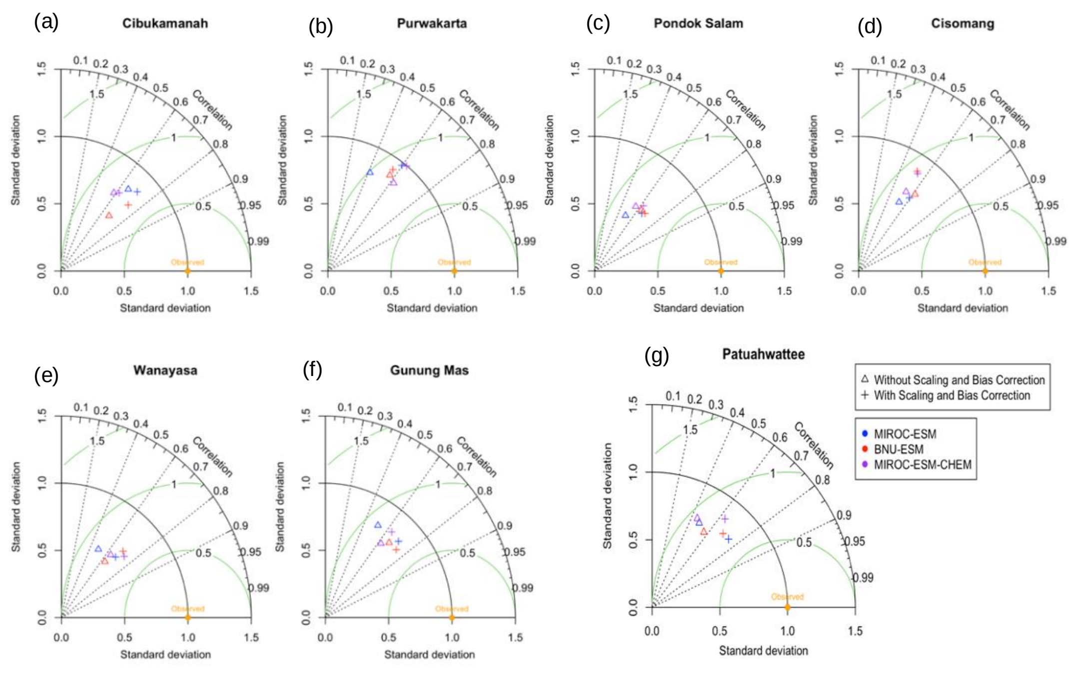

Figure 4. Taylor diagrams for evaluating TCPG-LASSO performance at seven rainfall stations in West Java: (a) Cibukamanah, (b) Purwakarta, (c) Pondok Salam, (d) Cisomang, (e) Wanayasa, (f) Gunung Mas, and (g) Patuahwattee.

The TCPG-LASSO model performs relatively well at Pondok Salam, Wanayasa, Gunung Mas, and Patuahwattee stations, where several model points are positioned closer to the observation reference. In contrast, the performance at Purwakarta is less satisfactory, as the model points are farther from the observation point compared with other stations. This suggests that local rainfall characteristics at Purwakarta may be more difficult to capture using the selected ESM predictors, possibly due to stronger local variability or weaker correspondence between ESM grid information and station rainfall.

Among the evaluated ESMs, BNU-ESM generally shows better performance in approximating local rainfall, as indicated by its position closer to the observation point in several stations. The results also show that TCPG-LASSO with scaling and bias correction produces better agreement with observed rainfall than the uncorrected scenario. Therefore, the corrected ESM outputs are more suitable for subsequent SPI projection. Based on this evaluation, the best-performing ESM model and treatment were selected for drought assessment in West Java.

Figure 5 compares the observed and predicted monthly rainfall during the testing period for the seven rainfall stations. The colours represent the ESM predictors, while the line types indicate the modelling scenarios, namely without scaling and bias correction and with scaling and bias correction. In general, the TCPG-LASSO model with scaling and bias correction is able to follow the seasonal pattern of observed rainfall, especially the wet-season peaks and dry-season decreases. This indicates that the combination of climate imprint rescaling and ISIMIP bias correction helps reduce the discrepancy between coarse ESM outputs and local station rainfall.

The model performance varies among stations. The predicted rainfall pattern is relatively close to the observed data at Wanayasa, Gunung Mas, and Patuahwattee, where the corrected TCPG-LASSO results are able to capture the main seasonal fluctuations. At several stations, the model without scaling and bias correction tends to overestimate rainfall during some wet months and shows larger deviations from the observed pattern. This suggests that using raw ESM outputs directly in the downscaling process may not be sufficient to represent local rainfall variability. Among the three ESMs, BNU-ESM generally shows a closer pattern to the observed rainfall, which is consistent with previous studies showing its ability to represent climate variability over the Indonesian region [9], [29].

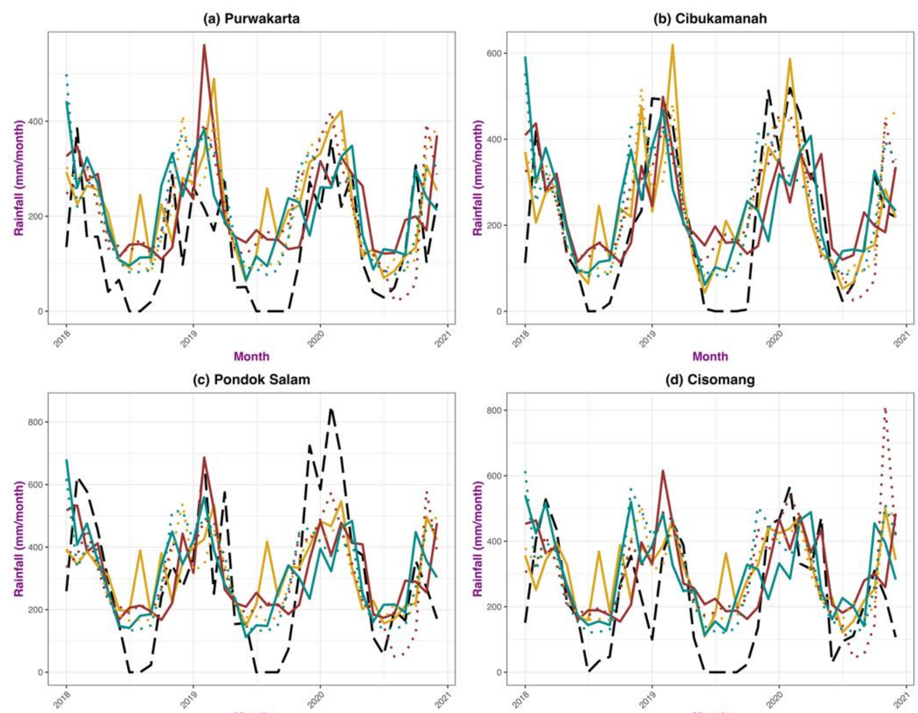

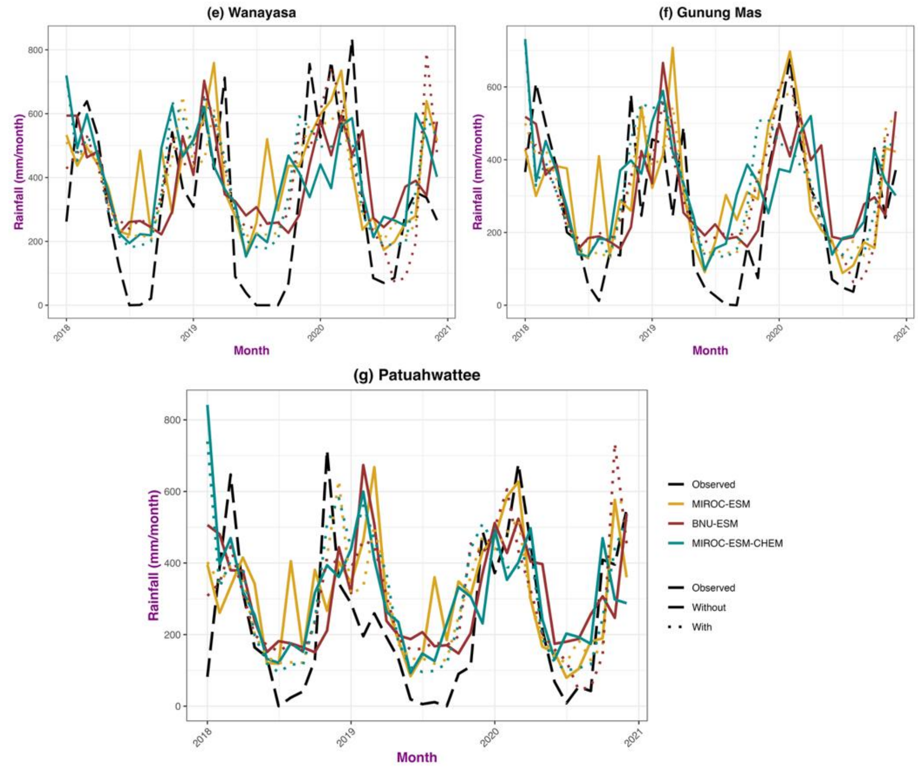

Figure 5. Time series plots of observed and predicted monthly rainfall during the testing period (January 2018–December 2020) at seven rainfall stations in West Java: (a) Purwakarta, (b) Cibukamanah, (c) Pondok Salam, (d) Cisomang, (e) Wanayasa, (f) Gunung Mas, and (g) Patuahwattee. The plots compare TCPG-LASSO predictions from three ESMs under two scenarios: without scaling and bias correction and with scaling and bias correction.

These results support the use of TCPG-LASSO for rainfall downscaling because rainfall data commonly contain zero or very low values and have a positively skewed, non-negative distribution [17]. Previous work by Hayati and Permatasari [20] also showed that the TCPG approach performs better than the Gamma-GLM method for rainfall modelling based on RMSEP. In this study, the integration of TCPG-LASSO with ESM rescaling and bias correction improves the agreement between predicted and observed rainfall. Compared with previous statistical downscaling and bias correction work, which produced an average correlation of around 0.5 [29], the proposed framework produces an average correlation of about 0.7. This improvement indicates that combining distribution-aware rainfall modelling with bias-corrected ESM information can improve local rainfall prediction.

Standardized Precipitation Index (SPI)

SPI is an index used to monitor drought and excessive rainfall based on precipitation anomalies. West Java is one of the important agricultural regions in Indonesia, so monitoring seasonal rainfall conditions is essential to support agricultural planning, water resource management, and hydrometeorological disaster mitigation. In this study, the SPI-6 projection was calculated using the best-performing ESM model, namely BNU-ESM, to assess future dry and wet conditions at seven rainfall stations in West Java.

Figure 6 shows that the projected SPI-6 values at most stations fluctuate mainly between -1 and 1, indicating that normal conditions dominate during the 2021–2030 period. However, several periods show clear departures from normal conditions, both toward dry and wet categories. Negative SPI-6 values appear repeatedly at different stations, suggesting the occurrence of accumulated rainfall deficits over several months. These dry conditions are visible around 2022, 2025–2027, and near 2029–2030, although the timing and intensity differ among stations.

The projected drought conditions are not spatially uniform across the seven stations. Purwakarta and Cibukamanah generally show moderate fluctuations, with most SPI-6 values remaining close to the normal range. In contrast, Pondok Salam, Wanayasa, Gunung Mas, and Patuahwattee show stronger variability, with several periods approaching severe dry or very wet conditions. Patuahwattee shows one of the most pronounced negative SPI-6 values near the end of the projection period, indicating a stronger accumulated rainfall deficit compared with the other stations.

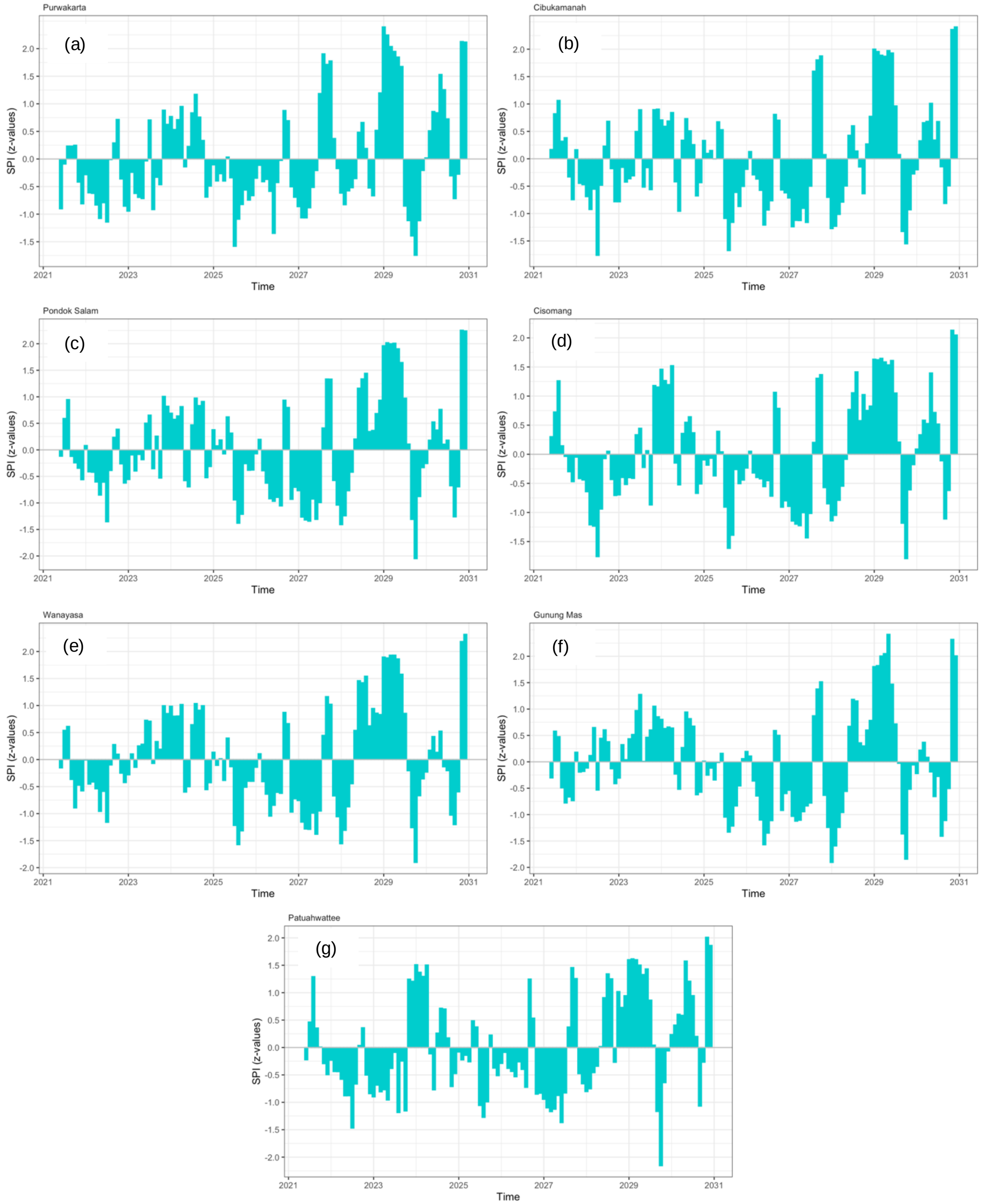

Figure 6. SPI-6 projections for seven rainfall stations in West Java based on the BNU-ESM model during 2021–2030: (a) Purwakarta, (b) Cibukamanah, (c) Pondok Salam, (d) Cisomang, (e) Wanayasa, (f) Gunung Mas, and (g) Patuahwattee.

The figure also indicates that wet conditions occur in several periods, particularly around 2028–2029 and toward the end of 2030. At some stations, SPI-6 values exceed 1 and approach very wet conditions, showing that rainfall anomalies in West Java are not limited to drought but also include excessive rainfall episodes. This alternating pattern between dry and wet conditions suggests that future rainfall variability may become more dynamic, with relatively rapid transitions from rainfall deficit to rainfall surplus.

These findings have practical implications for agricultural and disaster-risk planning in West Java. Periods with negative SPI-6 values may indicate increased drought risk, which can affect water availability, planting schedules, and crop productivity. Conversely, periods with high positive SPI-6 values may increase the risk of excessive rainfall, flooding, and landslides. Therefore, even though normal conditions remain dominant, the projected dry and wet episodes should be considered in early warning systems and seasonal climate-risk management.

Table 5 shows that the projected SPI-6 conditions in West Java were predominantly classified as normal. Of the 805 valid station-month occurrences, 583 (72.4%) were classified as normal, confirming the dominance of normal seasonal rainfall conditions during the projection period. Dry conditions accounted for 102 occurrences, comprising 85 moderately dry, 15 severely dry, and 2 extremely dry occurrences. Moderately dry conditions occurred at all stations and were most frequent at Pondok Salam and Gunung Mas, with 14 occurrences each, followed by Cisomang and Wanayasa, with 13 occurrences each. The two extremely dry occurrences were projected at Pondok Salam and Patuahwattee. These results indicate that several locations may experience seasonal rainfall deficits that could affect agricultural activities.

The occurrence of moderately dry conditions should be considered carefully because rainfall deficits can reduce soil moisture availability and affect crop growth. SPI conditions in the moderately dry category may reduce plant productivity and lead to yield losses [44], [45]. Similar evidence has been reported in agricultural studies showing that drought during the vegetable growing season can significantly reduce crop yields [46]. In particular, moderately dry SPI conditions during sensitive crop-growth phases, such as cauliflower formation, may have a negative impact on yield performance [45], [47].

Table 5. Number of projected SPI-6 category occurrences at each rainfall station in West Java from June 2021 to December 2030 based on the BNU-ESM model.

Station	Category of SPI						
	Extremely dry	Severely dry	Moderately dry	Normal	Moderately wet	Very wet	Extremely wet
Purwakarta	0	2	9	88	4	7	5
Cibukamanah	0	3	11	88	2	8	3
Pondok Salam	1	0	14	85	7	5	3
Cisomang	0	3	13	76	14	7	2
Wanayasa	0	3	13	83	7	7	2
Gunung Mas	0	4	14	83	5	7	2
Patuahwattee	1	0	11	80	16	6	1
Total	**2**	**15**	**85**	**583**	**55**	**47**	**18**

Wet conditions accounted for 120 occurrences, comprising 55 moderately wet, 47 very wet, and 18 extremely wet occurrences. Moderately wet conditions were most frequent at Patuahwattee, with 16 occurrences, followed by Cisomang, with 14 occurrences. Purwakarta recorded the highest number of extremely wet occurrences, with five occurrences. These results show that projected rainfall-related risks are not limited to drought but also include excessive rainfall. Very wet and extremely wet conditions may increase the risk of flooding, waterlogging, and other hydrometeorological hazards. Therefore, both dry and wet SPI-6 anomalies should be considered in agricultural planning and climate-risk management.

Although normal conditions remain dominant, repeated occurrences of moderately dry, severely dry, and extremely dry conditions indicate that drought risk should not be ignored. At the same time, the occurrence of very wet and extremely wet conditions indicates that seasonal rainfall surplus may also become an important concern. These findings can be used as a reference for local governments and agricultural stakeholders in preparing early warning systems, adjusting planting calendars, and reducing the potential impacts of climate variability on crop production.

Conclusions

This study demonstrates that the integration of Tweedie Compound Poisson–Gamma (TCPG), Least Absolute Shrinkage and Selection Operator (LASSO), ESM resolution enhancement, and ISIMIP bias correction provides an effective framework for ESM-driven rainfall downscaling in West Java. The exploratory analysis confirms that rainfall at the seven stations follows a unimodal seasonal pattern, with higher rainfall during the wet months and lower rainfall during the dry months. The rainfall distribution is non-negative, positively skewed, and contains zero or near-zero values, supporting the use of the TCPG framework to represent both rainfall occurrence and rainfall intensity.

The incorporation of LASSO improves the downscaling model by selecting only the most relevant ESM grid predictors and reducing multicollinearity among spatially correlated grids. The selected number of grids was relatively small, indicating a sparse and computationally efficient predictor structure. This result shows that retaining all ESM grids is not necessary, because many neighbouring grids contain similar climate information. The penalty parameter was objectively determined using 10-fold cross-validation based on minimum deviance, ensuring that the selected predictors contribute meaningfully to model performance.

The model evaluation indicates that TCPG-LASSO with climate imprint rescaling and ISIMIP bias correction generally performs better than the uncorrected scenario. The corrected model is better able to follow the seasonal pattern of observed rainfall, particularly the wet-season peaks and dry-season decreases. Among the three evaluated ESMs, BNU-ESM shows the most consistent performance in representing local rainfall variability and was therefore selected as the basis for SPI-6 projection. The proposed framework improves the agreement between observed and predicted rainfall, with an average correlation of about 0.7, indicating better performance than previous statistical downscaling and bias correction approaches reported for Indonesia.

The SPI-6 projection based on BNU-ESM shows that normal seasonal rainfall conditions remain dominant in West Java during 2021–2030. Based on 805 valid station-month SPI-6 values from June 2021 to December 2030, 583 occurrences were classified as normal. Nevertheless, the projection also indicates dry anomalies comprising 85 moderately dry, 15 severely dry, and 2 extremely dry occurrences, as well as wet anomalies comprising 55 moderately wet, 47 very wet, and 18 extremely wet occurrences. These results suggest that future rainfall variability in West Java is not limited to drought risk but also includes excessive-rainfall risk. Therefore, both accumulated rainfall deficits and rainfall surpluses should be considered in agricultural planning, water-resource management, and hydrometeorological disaster mitigation.

Overall, this study confirms that TCPG-LASSO combined with ESM resolution enhancement and ISIMIP bias correction is a useful methodological framework for translating coarse-scale ESM information into local rainfall projections. The results provide practical information for local governments and agricultural stakeholders in developing early warning systems, adjusting planting calendars, and reducing the potential impacts of future climate variability on crop production and hydrometeorological risk in West Java.

Conflicts of Interest

The authors declare that there is no conflict of interest regarding the publication of this paper.

Acknowledgment

The authors gratefully acknowledge financial support from the Institute for Research and Community Service (LPPM), Universitas Muhammadiyah Semarang, through the Internal Grant (Lecturer Beginner Scheme), Fiscal Year 2024, under Contract No. 0138/UNIMUS.L/PG/PJ.INT/2024.

References

[1] J. A. Marengo, L. M. Alves, T. Ambrizzi, A. Young, N. J. C. Barreto, and A. M. Ramos, “Trends in extreme rainfall and hydrogeometeorological disasters in the Metropolitan Area of São Paulo: a review,” *Ann. N. Y. Acad. Sci.*, vol. 1472, no. 1, pp. 5–20, Jul. 2020, doi: https://doi.org/10.1111/nyas.14307.

[2] J. T. Nugroho, D. Nurfitriani, Suwarsono, G. A. Chulafak, R. J. Manalu, and S. Harini, “Rainfall anomalies assessment during drought episodes of 2015 in Indonesia using CHIRPS Data,” in *IOP Conference Series: Earth and Environmental Science*, IOP Publishing Ltd, Apr. 2021. doi: 10.1088/1755-1315/739/1/012044.

[3] I. Purnamasari, T. Wahyu Saputra, and S. Ristiyana, “Pola Spasial Kekeringan di Jawa Barat Pada Kondisi El Nino Berbasis Metode Palmer Drought Severity Index (PDSI),” *Jurnal Teknik Pengairan*, vol. 12, no. 1, pp. 16–29, May 2021, doi: 10.21776/ub.pengairan.2021.012.01.02.

[4] W. Kim, T. Iizumi, and M. Nishimori, “Global patterns of crop production losses associated with droughts from 1983 to 2009,” *J. Appl. Meteorol. Climatol.*, vol. 58, no. 6, pp. 1233–1244, 2019, doi: 10.1175/JAMC-D-18-0174.1.

[5] A. Maiti *et al.*, “Optimal rainfall threshold for monsoon rice production in India varies across space and time,”

Commun. Earth Environ., vol. 5, no. 1, Dec. 2024, doi: 10.1038/s43247-024-01414-7.

[6] C. Tebaldi *et al.*, "Climate model projections from the Scenario Model Intercomparison Project (ScenarioMIP) of CMIP6," *Earth System Dynamics*, vol. 12, no. 1, pp. 253–293, Mar. 2021, doi: 10.5194/esd-12-253-2021.

[7] F. Fauzi, H. Kuswanto, and R. M. Atok, "Bias correction and statistical downscaling of earth system models using quantile delta mapping (QDM) and bias correction constructed analogues with quantile mapping reordering (BCCAQ)," in *Journal of Physics: Conference Series*, 2020. doi: 10.1088/1742-6596/1538/1/012050.

[8] B. Miftahurrohmah, H. Kuswanto, D. S. Pambudi, F. Fauzi, and F. Atmaja, "Assessment of the Support Vector Regression and Random Forest Algorithms in the Bias Correction Process on Temperatures," in *Procedia Computer Science*, Elsevier B.V., 2024, pp. 637–644. doi: 10.1016/j.procs.2024.03.049.

[9] H. Kuswanto, B. Kravitz, B. Miftahurrohmah, F. Fauzi, A. Sopahaluwaken, and J. Moore, "Impact of solar geoengineering on temperatures over the Indonesian Maritime Continent," *International Journal of Climatology*, no. August 2020, pp. 1–20, 2021, doi: 10.1002/joc.7391.

[10] A. Casanueva, S. Kotlarski, S. Herrera, A. M. Fischer, T. Kjellstrom, and C. Schwierz, "Climate projections of a multivariate heat stress index: The role of downscaling and bias correction," *Geosci. Model Dev.*, vol. 12, no. 8, pp. 3419–3438, 2019, doi: 10.5194/gmd-12-3419-2019.

[11] R. Manzanas, A. Lucero, A. Weisheimer, and J. M. Gutiérrez, "Can bias correction and statistical downscaling methods improve the skill of seasonal precipitation forecasts?," *Clim. Dyn.*, vol. 50, no. 3, pp. 1161–1176, 2018, doi: 10.1007/s00382-017-3668-z.

[12] Y. Tong, X. Gao, Z. Han, Y. Xu, Y. Xu, and F. Giorgi, "Bias correction of temperature and precipitation over China for RCM simulations using the QM and QDM methods," *Clim. Dyn.*, vol. 57, pp. 1425–1443, 2021, doi: 10.1007/s00382-020-05447-4.

[13] D. Sandler, H. Saaroni, B. Ziv, A. Hochman, N. Harnik, and D. Rostkier-Edelstein, "A multiscale approach to statistical downscaling of daily precipitation: Israel as a test case," *International Journal of Climatology*, vol. 44, no. 1, pp. 59–71, Jan. 2024, doi: 10.1002/joc.8315.

[14] S. S. Sami, A. A. Ali, and A. D. Jalal, "An application of the statistical downscaling model (SDSM) to simulate precipitation data in the Iraqi Western Desert," *AIP Conf. Proc.*, vol. 3009, no. 1, p. 030113, Feb. 2024, doi: 10.1063/5.0197996.

[15] P. K. Dunn and G. K. Smyth, "Series evaluation of Tweedie exponential dispersion model densities," *Stat. Comput.*, vol. 15, no. 4, pp. 267–280, 2005, doi: 10.1007/s11222-005-4070-y.

[16] W. H. Bonat and C. C. Kokonendji, "Flexible Tweedie regression models for continuous data," *J. Stat. Comput. Simul.*, vol. 87, no. 11, pp. 2138–2152, Jul. 2017, doi: 10.1080/00949655.2017.1318876.

[17] N. C. Dzupire, P. Ngare, and L. Odongo, "A Poisson-Gamma Model for Zero Inflated Rainfall Data," *J. Probab. Stat.*, vol. 2018, no. 1, pp. 1–12, 2018, doi: 10.1155/2018/1012647.

[18] D. Dewanti, A. Djuraidah, B. Sartono, and A. Sopaheluwakan, "Bias correction and ensemble techniques in statistical downscaling model for rainfall prediction using Tweedie-LASSO in West Java, Indonesia," *Journal of Agrometeorology*, vol. 26, no. 3, pp. 324–330, Sep. 2024, doi: 10.54386/jam.v26i3.2614.

[19] M. Hayati, A. H. Wigena, A. Djuraidah, and A. Kurnia, "A new approach to statistical downscaling using tweedie compound poisson gamma response and lasso regularization," *Communications in Mathematical Biology and Neuroscience*, vol. 2021, 2021, doi: 10.28919/cmbn/5936.

[20] M. Hayati and R. Permatasari, "Comparison of Generalized Linear Model between Gamma and Tweedie Compound Response for Rainfall Prediction in Lampung Province," *Asian Journal of Probability and Statistics*, vol. 26, no. 1, pp. 41–49, Jan. 2024, doi: 10.9734/ajpas/2024/v26i1583.

[21] A. Arisandi, A. H. Wigena, and A. Mohamad Soleh, "Continuum Regression Modeling with LASSO to Estimate Rainfall," *International Journal of Scientific and Research Publications (IJSRP)*, vol. 10, no. 10, pp. 380–385, Oct. 2020, doi: 10.29322/ijsrp.10.10.2020.p10651.

[22] R. N. Rachmawati, I. Sungkawa, and A. Rahayu, "Extreme Rainfall Prediction using Bayesian Quantile Regression in Statistical Downscaling Modeling," *Procedia Comput. Sci.*, vol. 157, pp. 406–413, 2019, doi: https://doi.org/10.1016/j.procs.2019.08.232.

[23] R. R. He, Y. Chen, Q. Huang, and Y. Kang, "LASSO as a tool for downscaling summer rainfall over the Yangtze River Valley," *Hydrological Sciences Journal*, vol. 64, no. 1, pp. 92–104, Jan. 2019, doi: 10.1080/02626667.2019.1570210.

[24] W. Qian and H. H. Chang, "Projecting health impacts of future temperature: A comparison of quantile-mapping bias-correction methods," *Int. J. Environ. Res. Public Health*, vol. 18, no. 4, pp. 1–12, Feb. 2021, doi: 10.3390/ijerph18041992.

[25] P. Dhawan *et al.*, "A comprehensive comparison of bias correction methods in climate model simulations: Application on ERA5-Land across different temporal resolutions," *Heliyon*, vol. 10, no. 23, Dec. 2024, doi: 10.1016/j.heliyon.2024.e40352.

[26] A. J. Cannon, S. R. Sobie, and T. Q. Murdock, "Bias correction of GCM precipitation by quantile mapping: How well do methods preserve changes in quantiles and extremes?," *J. Clim.*, vol. 28, no. 17, pp. 6938–6959, 2015, doi: 10.1175/JCLI-D-14-00754.1.

[27] A. T. Werner and A. J. Cannon, "Hydrologic extremes -- an intercomparison of multiple gridded statistical downscaling methods," *Hydrol. Earth Syst. Sci.*, vol. 20, no. 4, pp. 1483–1508, 2016, doi: 10.5194/hess-20-1483-2016.

[28] S. Lange, "Trend-preserving bias adjustment and statistical downscaling with ISIMIP3BASD (v1.0)," *Geosci. Model Dev.*, vol. 12, no. 7, pp. 3055–3070, 2019, doi: 10.5194/gmd-12-3055-2019.

[29] F. Fauzi, H. Kuswanto, R. M. Atok, and M. Salamah, "Statistical Downscaling and Bias Correction of the Earth System Models (ESM) Outputs for Future Climate Projection under Solar Geoengineering : Case Study Indonesia," *Journal of Mechanical Engineering*, vol. 10, no. 1, pp. 33–49, 2021.

[30] G. A. Meehl *et al.*, "Climate System Response to External Forcings and Climate Change Projections in CCSM4," *J. Clim.*, vol. 25, no. 11, pp. 3661–3683, 2012, doi: https://doi.org/10.1175/JCLI-D-11-00240.1.

[31] D. Ji *et al.*, "Description and basic evaluation of Beijing Normal University Earth System Model (BNU-ESM)

version 1," *Geosci. Model Dev.*, vol. 7, no. 5, pp. 2039–2064, Sep. 2014, doi: 10.5194/gmd-7-2039-2014.

[32] S. Watanabe *et al.*, "MIROC-ESM 2010: Model description and basic results of CMIP5-20c3m experiments," *Geosci. Model Dev.*, vol. 4, no. 4, pp. 845–872, 2011, doi: 10.5194/gmd-4-845-2011.

[33] R. D. Hunter and R. K. Meentemeyer, "Climatologically Aided Mapping of Daily Precipitation and Temperature," *Journal of Applied Meteorology*, vol. 44, pp. 1501–1510, 2005.

[34] S. Hempel, K. Frieler, L. Warszawski, J. Schewe, and F. Piontek, "A trend-preserving bias correction – the ISI-MIP approach," *Earth Syst. Dynam.*, vol. 4, no. 2, pp. 219–236, 2013, doi: 10.5194/esd-4-219-2013.

[35] F. Saeed *et al.*, "Bias correction of multi-ensemble simulations from the HAPPI model intercomparison project," *Geoscientific Model Development Discussions*, vol. 2018, pp. 1–23, 2018, doi: 10.5194/gmd-2018-107.

[36] I. Macadam, D. Argüeso, J. P. Evans, D. L. Liu, and A. J. Pitman, "The effect of bias correction and climate model resolution on wheat simulations forced with a regional climate model ensemble," *International Journal of Climatology*, vol. 36, no. 14, pp. 4577–4591, Nov. 2016, doi: https://doi.org/10.1002/joc.4653.

[37] Q. Zhou, D. Chen, Z. Hu, and X. Chen, "Decompositions of Taylor diagram and DISO performance criteria," *International Journal of Climatology*, vol. 41, no. 12, pp. 5726–5732, Oct. 2021, doi: https://doi.org/10.1002/joc.7149.

[38] Z. Xu and Y. Han, "Short communication comments on 'DISO: A rethink of Taylor diagram,'" *International Journal of Climatology*, vol. 40, no. 4, pp. 2506–2510, Mar. 2020, doi: https://doi.org/10.1002/joc.6359.

[39] A. Faisol, I. Indarto, E. Novita, and B. Budiyono, "Assessment of agricultural drought based on CHIRPS data and SPI method over West Papua – Indonesia," *Journal of Water and Land Development*, vol. 52, pp. 44–52, 2022, doi: 10.24425/jwld.2021.139942.

[40] M. Ariska, Suhadi, Supari, M. Irfan, and I. Iskandar, "Detection of Dominant Rainfall Patterns in Indonesian Regions Using Empirical Orthogonal Function (EOF) and Its Relation with ENSO and IOD Events," *Science and Technology Indonesia*, vol. 9, no. 4, pp. 1009–1023, Oct. 2024, doi: 10.26554/sti.2024.9.4.1009-1023.

[41] M. Yustiana, M. Zainuri, D. N. Sugianto, M. P. N. Batubara, and A. M. Hidayat, "Dampak Variabilitas Iklim Inter-Annual (El Niño, La Niña) Terhadap Curah Hujan dan Anomali Tinggi Muka Laut di Pantai Utara Jawa Tengah," *Buletin Oseanografi Marina*, vol. 12, no. 1, pp. 109–124, Feb. 2023, doi: 10.14710/buloma.v12i1.48377.

[42] P. K. Dunn and G. K. Smyth, *Generalized Linear Models With Examples in R*. Springer, 2018.

[43] K. E. Taylor, "Summarizing multiple aspects of model performance in a single diagram," *J. Geophys. Res.*, vol. 106, no. D7, pp. 7183–7192, 2001.

[44] K. Hussain and M. Shahab, "An Investigation Standardized Precipitation Index Trend in Arid and Semi-arid Region of Pakistan Applying the Innovative Trend Analysis (ITA) Technique," in *Water Resources in Arid Lands: Management and Sustainability*, A. Al-Maktoumi, O. Abdalla, A. Kacimov, S. Zekri, M. Chen, T. Al-Hosni, and K. Madani, Eds., Cham: Springer International Publishing, 2021, pp. 111–120.

[45] A. Gholinia and P. Abbaszadeh, "Agricultural Drought Monitoring: A Comparative Review of Conventional and Satellite-Based Indices," Sep. 01, 2024, *Multidisciplinary Digital Publishing Institute (MDPI)*. doi: 10.3390/atmos15091129.

[46] V. Potop, M. Možný, and J. Soukup, "Drought evolution at various time scales in the lowland regions and their impact on vegetable crops in the Czech Republic," *Agric. For. Meteorol.*, vol. 156, pp. 121–133, 2012, doi: https://doi.org/10.1016/j.agrformet.2012.01.002.

[47] M. Santini, S. Noce, M. Antonelli, and L. Caporaso, "Complex drought patterns robustly explain global yield loss for major crops," *Sci. Rep.*, vol. 12, no. 1, Dec. 2022, doi: 10.1038/s41598-022-09611-0.